Analyze and evaluate of energy management system for fuel cell electric vehicle based on frequency splitting

Abderrezak Badji, Djaffar Ould Abdeslam, Mohamed Becherif, Fouad Eltoumi, Nacereddine Benamrouche

Version of Record: https://www.sciencedirect.com/science/article/pii/S0378475419300722
Manuscript_977814e2d54b0a853ee8e023eb2e03a1

Analyze and Evaluate of Energy Management System for Fuel Cell Electric Vehicle based on Frequency Splitting

Abderrezak Badji[a,b,*], Djaffar Ould Abdeslam[b], Mohamed Becherif[c], Fouad Eltoumi[c], Nacereddine Benamrouche[a]

[a] *LATAGE Laboratory, Mouloud Mammeri University of Tizi-Ouzou, BP 17 RP 15000 Tizi-Ouzou, Algeria*
[b] *IRIMAS Laboratory, Haute Alsace University, 61 rue Albert Camus 68093 Mulhouse, France*
[c] *FCLab FR CNRS 3539, Femto-ST UMR CNRS 6174, Univ. Bourgogne Franche-Comté/UTBM, 90010 Belfort, France*

Abstract

This paper presents a control strategy for hybrid power source based on fuel cell (FC) as the main power source and battery/supercapacitor (SC) as auxiliary power sources for electric vehicle application. In this study, a Battery and SC are auxiliary devices associated with the FC to ensure the power reversibility in the drive train. The FC, Battery, and SC are connected to the DC bus throughout an interleaved boost converter (IBC) and two interleaved bidirectional converters (IBDC) respectively. The paper proposes the control strategy based on power frequency splitting to avoid FC starvation problem, reduce the battery stress and improve the fuel economy of FC. The detail of the control strategy is presented and an Energetic Macroscopic Representation (EMR) is used to develop the whole system. The simulation results are presented to validate the proposed method in the hybrid system.

Keywords:
Fuel cell (FC), Electric Vehicle (EV), Hybrid Electric Vehicle (HEV), Energy Management System (EMS), Energetic Macroscopic Representation (EMR)

1. Introduction

In the last few years, fuel cells (FCs) have gained a growing interest for power generation both for stationary and transportation applications. FCs are electrochemical devices that convert chemical energy directly from an oxygen and hydrogen reaction into electrical energy releasing water and heat, providing quietness of operation, reliability and enabling zero-emission transportation [1, 2, 3, 4]. Therefore, hydrogen FCs are considered as a potential propulsion technology for automotive transportation. But, despite the importance of these technologies in reducing the environmental impact, many issues that have to be overcome

*Corresponding author
Email address: badji_ummto@yahoo.com (Abderrezak Badji)

are studied, such as FC stacks (membrane, catalyst) [5, 6], main subsystems including air compressor [7], hydrogen storage and distributing infrastructure [8] and vehicle integration [9]. Indeed, the FC conditions for use are investigated regarding the vehicle requirements, such as FC lifetime and failure recovery [10], low dynamics and decreasing of efficiency at high current density [11].

Among the existing technologies of FCs, proton exchange membrane fuel cell (PEMFC) seems to be a potential candidate for vehicle applications thanks to its: (1) high power density and solid electrolyte[12, 13, 14]; (2) lower operation temperature, which makes them rapidly turned on and off; (3) lower operation pressure (which guarantees greater safety); (4) easily setting into mode system; (5) lower emission ratio and (6) higher conversion ratio [3, 13]. Furthermore, the slow response of the FC impacts on vehicle performances. At present, no single energy-storage device could meet all requirements of hybrid electric vehicles HEVs and electric vehicles (EVs). Besides, hybrid energy sources complement drawbacks of a single device [14, 15]. As a result, FCs must be combined with, at least, an intermediate energy storage element that possesses sufficient energy. They should also be able to deliver large amounts of power. Previous research showed that using FC hybridization with a battery or a supercapacitor (SC) results in reducing cost and fuel consumption reduction as well as in improving the performance of EV [16, 17, 18].

In fact, the very high capacitance of SCs comes at a cost. The operating voltage of a SC cell cannot exceed the potential at which the electrolyte undergoes chemical reactions (typically [2.5–3]V per cell). For high voltage applications, SC cells, can be series-connected. One of the most important advantages of batteries over SC is their high energy density. Indeed, the amount of charge they can charge (3–30) times greater than that stored by SCs. However, SCs can deliver hundreds to many thousands times the power of a similar sized battery. Besides, the highly-reversible electrostatic charge storage in SCs does produce changes in the volume that usually accompanies the redox reactions of the active masses in batteries. Such volume changes are the main causes of the limited cycle life of batteries (around 1000 cycles for a lead-acid battery), compared to the charge–discharge cycles for SCs [13, 17, 19].

These electrochemical systems admit a varied combination between the FC, battery and SC. Depending on the topology, the power management may change. For example, for the FC/Battery case, the battery will be under severe power bursts [20], which could shorten the battery life time. The FC/SC combination could improve the life time, because SCs present higher power, more ramp capability than batteries [21]. However, SCs are characterized by much lower energy density than batteries [17]. They could also cause problems related to during vehicle start-up [22]. The B/SC combination could solve this last aspect, but it will reduce the total energy density due to the fact that batteries have a lower energy density than FCs [23]. Therefore, the FC/Battery/SC combination keeps its higher energy density due to the FC. The high power density and ramp capability due to the implementation of SC and batteries, as studied by Thounthong et all [19]. This combination is based on using the FC, battery and SC by taking account of the intrinsic energetic characteristics of these sources. C.H. Zheng et all. [24], already proposed a strategy of fuel economy evaluation based on the equivalent fuel consumption without taking into account the dynamic of the

FC. Premananda Pany et all [25], proposed a strategy of Active load current sharing without controlling the State of Charge (SOC) of battery and FC consumption.

This paper propose an energy management system (EMS) for a hybrid FC Battery/SC power source. The proposed system model and the control structure are depicted using energetic macroscopic representation (EMR). The applied control strategy is based on power frequency splitting in order to protect the hybrid sources, and improves the fuel economy of FC. This paper is organized as follows: In Section Hybrid electric vehicle configuration, the topology of the electrical system for FCHEV is discussed, including the interleaving technic of the converters. The energy flows analysis of the hybrid system, and the reference power for every source is studied in Section Energy management system for hybrid electric vehicle. EMR, modeling and control of power converters are presented in section IV. In Section Results and discussion, simulation results of the proposed strategy are presented, considering hydrogen consumption and SOCs of Battery/SC. Finally, the conclusions are summarized in Section Conclusion.

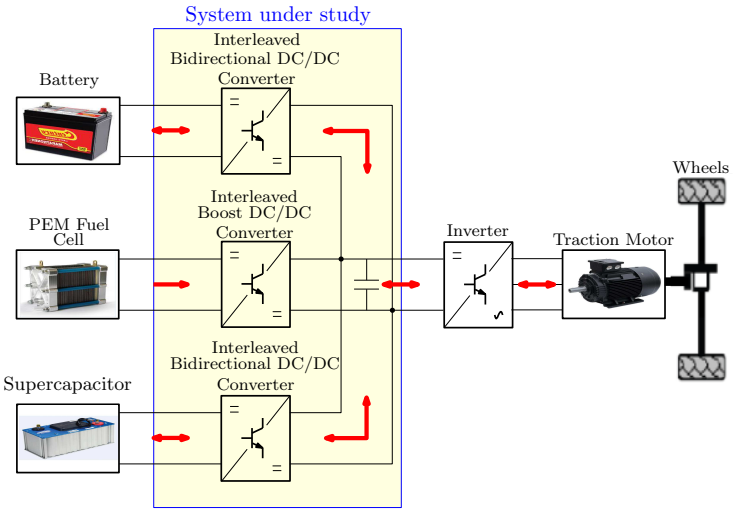

Figure 1: Proposed structure of the FC/battery/SC hybrid power source

2. Hybrid electric vehicle configuration

The configuration of the traction system of the FCEV is illustrated in (Figure. 1). This system is composed of the FC which represents the main power source connected to the DC bus through unidirectional boost converter, and the auxiliary power sources (battery and SC) connected to the same DC bus by two bidirectional converters to assist the propulsion of the vehicle during transients and to absorb the kinetic energy during regenerative braking. The presented topology is based on an interleaved boost converter (IBC) and two bidirectional converters (IBDC), (Figure. 2). The inductors of each converter are the same and independent ($L_1 = L_2 = L_3 = L$). These three converters have the same output capacitor. The interleaving technics are characterized by their high voltage step up, reduced the output

voltage ripple, reduced the input current ripple, low switching loss, reduced electromagnetic interference, fast transient response and continuity of service.

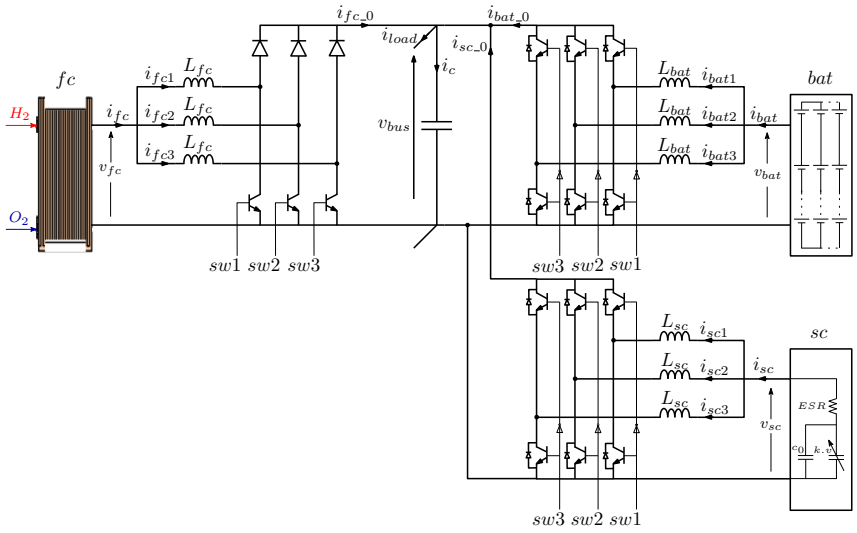

Figure 2: Schematic diagram of the proposed FCEV system

3. Energy management system for hybrid electric vehicles

The FCs for electric vehicle usually works under complex operating conditions, including start/stop and frequently changing load condition. This is the main reason why the durability of automotive FCs is shorter than that of the stationary ones. Thus, the performance of the FC can be improved by establishing a good energy distribution between the FC and the energy storage system (ESS). (Figure. 3) shows that fuel consumption (Hydrogen) is very high when the FC is operating in low and high power areas.

Furthermore, at low power zone, the FC efficiency is low because the power is used to supply the various components of the FC (compressors, valves...). It is also not elevated in the high power zone due to the nature of the FC system. From the curves shown in (Figure. 3) optimal exploitation zone of the FC in terms of efficiency and fuel consumption varies between (30 and 70) % of its maximum power. (Figure. 4) shows the different time response of the energy sources that must be taken into account when designing the control algorithm.

According to (Figure. 3) and (Figure. 4), the applied control strategy must ensure the optimal power flow between FC, Battery and SC. In this case, the FC must always be controlled in its medium power range by imposing a very slow dynamic and the power or the current flow must be limited to avoid the lack of fuel. The SC bank must be checked to satisfy all very fast transient demands and load peaks. The battery should be also checked for intermediate dynamics.

The EMS is developed as function of the balance of the system throughout the lifetime of the vehicle. The power produced by the FC is compared with the DC bus power (load

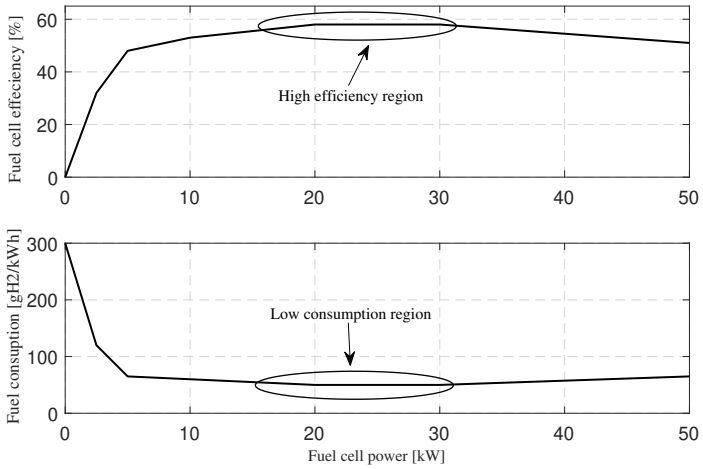

Figure 3: Fuel cell system efficiency and fuel consumption versus net power for the FC system

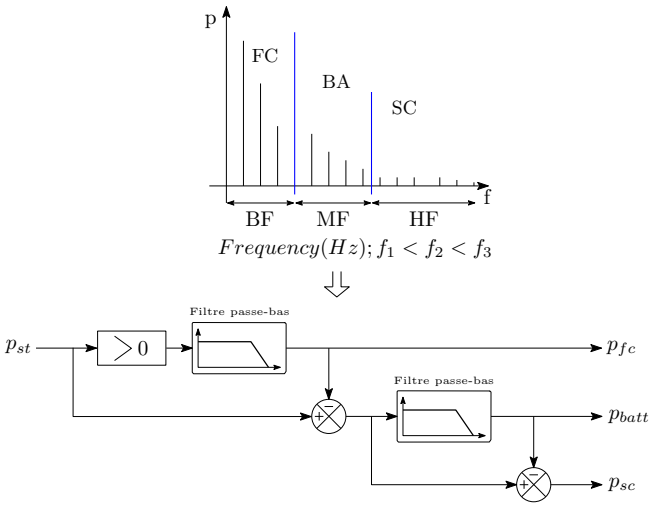

Figure 4: Strategy for power frequency splitting

power). This comparison determines the distribution of the energy flow between the storage elements and the DC bus.

The FC reference power is calculated by the following equation:

$$P_{fc} = \frac{1}{\eta(1+\tau_1 s)} P_{load} \tag{1}$$

Where P_{fc} represents the output net power of FC system, η corresponds to the EV system efficiency, and τ_1 denotes the filter time constant of FC.

To protect the battery during operation of the EV, the battery power must be corrected by considering a low pass filter. The SC and/or battery reference power (P^*_{net}) is calculated

by the following equation:

$$P_{net}^{*} = \frac{1}{\eta(1+\tau_2 s)} P_{net} \tag{2}$$

Where τ_2 denotes the filter time constant of the battery. The control process described in (Figure. 5) is detailed below

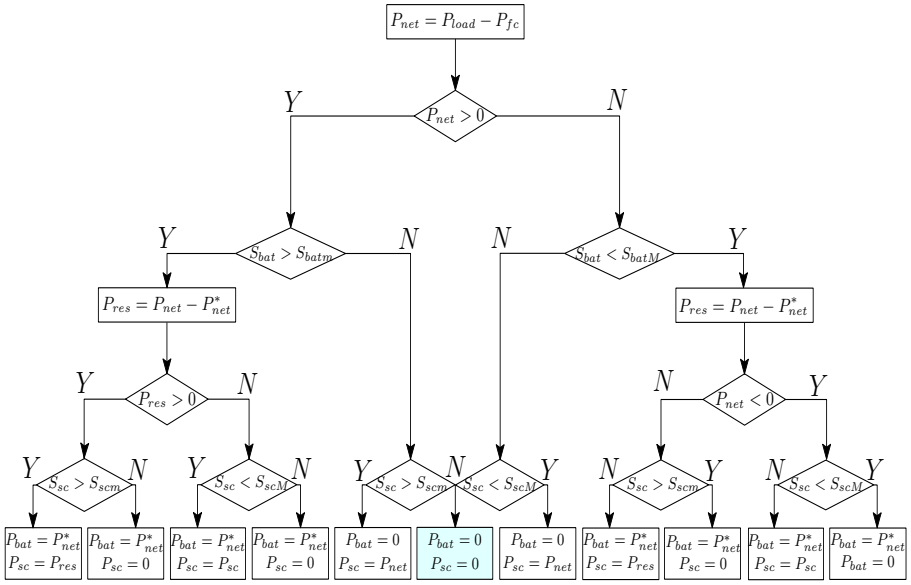

Figure 5: Power management control

If the power difference (P_{net}) is positive (excess power), the control system must transfer this excess to the storage system (Battery/SC) while respecting the dynamics and the limits of use of each storage source. If P_{net} is negative (deficit power), the control system must draw this lack of power from the storage system. The SOC of the battery and the SC must be known at driving mode. To guarantee a safety margin of the storage system with respect to the SOCs, the dimensioning of the elements was carried out with a discharge depth $k = 55\%$. Indeed, the proposed control strategy aims at finding an optimal trajectory of the power distribution between the three sources when the vehicle is in driving mode. From this strategy, the power references (P_{fc_ref}, P_{bat_ref}, and P_{sc_ref}) can be imposed to control three DC/DC converters.

4. EMR, modeling and control of power converters

The structure of the power converters and their control methods are represented by the Energetic Macroscopic Representation (EMR) shown in (Figure. 6). EMR is a graphic formalism for the synthetic representation of the multidisciplinary energy system. It leads to a functional description of an energy system. It also respects the integral causality of the studied system, which systematic deduction of a control structure. The maximum

control structure (SMC) can be defined from the EMR by inverting its elements [26]. From (Figure. 6), we notice the existence of a mirror effect between the SMC and the EMR.

The EMR is based on three main elements used to describe each component, source element, Accumulation element and Conversion element. The source element (green oval pictogram) has a single input or a set of vector defined quantities and only one output or output vector. Accumulation element (orange rectangular pictogram with slash) symbolizes the notion of temporal break between the input and output variables. The accumulation element can either be scalars or vectors. Indeed, the storage element stores energy internally (with or without loss). Thereby, in order to respect the integral causality, their outputs are integral functions entrances. Finally, in the Conversion element, there is no energy storage. The input and output variables are, therefore, not defined before being connected to other elements. Conversion elements are represented by orange square pictograms.

From the EMR of the system, we observe a control structure which consists of a maximum of control and measurement operations. This structure must reverse the overall function of the system. The principle of EMR inversion control is detailed in [26]. The global control structure is broken down into several control blocks; each one of which them be reversed directly from the EMR. The accumulation elements have controllers to solve the problem inverting their state variables. All control blocks are represented by blue parallelograms.

4.1. FC converter

The interleaved boost DC/DC converter, for which the output voltage is always higher than the FC voltage. In the diagram presented in (Figure. 6). A coupling element is introduced into the FC converter to indicate the energy distribution, it is represented by three intersected squares. This specific coupling device is associated with the following relations:

$$\begin{cases} v_{fc1} = v_{fc2} = v_{fc3} = v_{fc} \\ i_{fc1} + i_{fc2} + i_{fc3} = i_{fc} \end{cases} \tag{3}$$

The current of each inductance can be expressed as:

$$L_{fci}\frac{di_{fci}}{dt} = v_{fci} - v_{swi} \tag{4}$$

The modulation function of the interleaved boost converter can be expressed from the switching functions as follows:

$$\begin{cases} v_{bus} = \dfrac{1}{m_{fci}} v_{fci} \\ i_{fci} = \dfrac{1}{m_{fci}} i_{fci\_0} \end{cases} \tag{5}$$

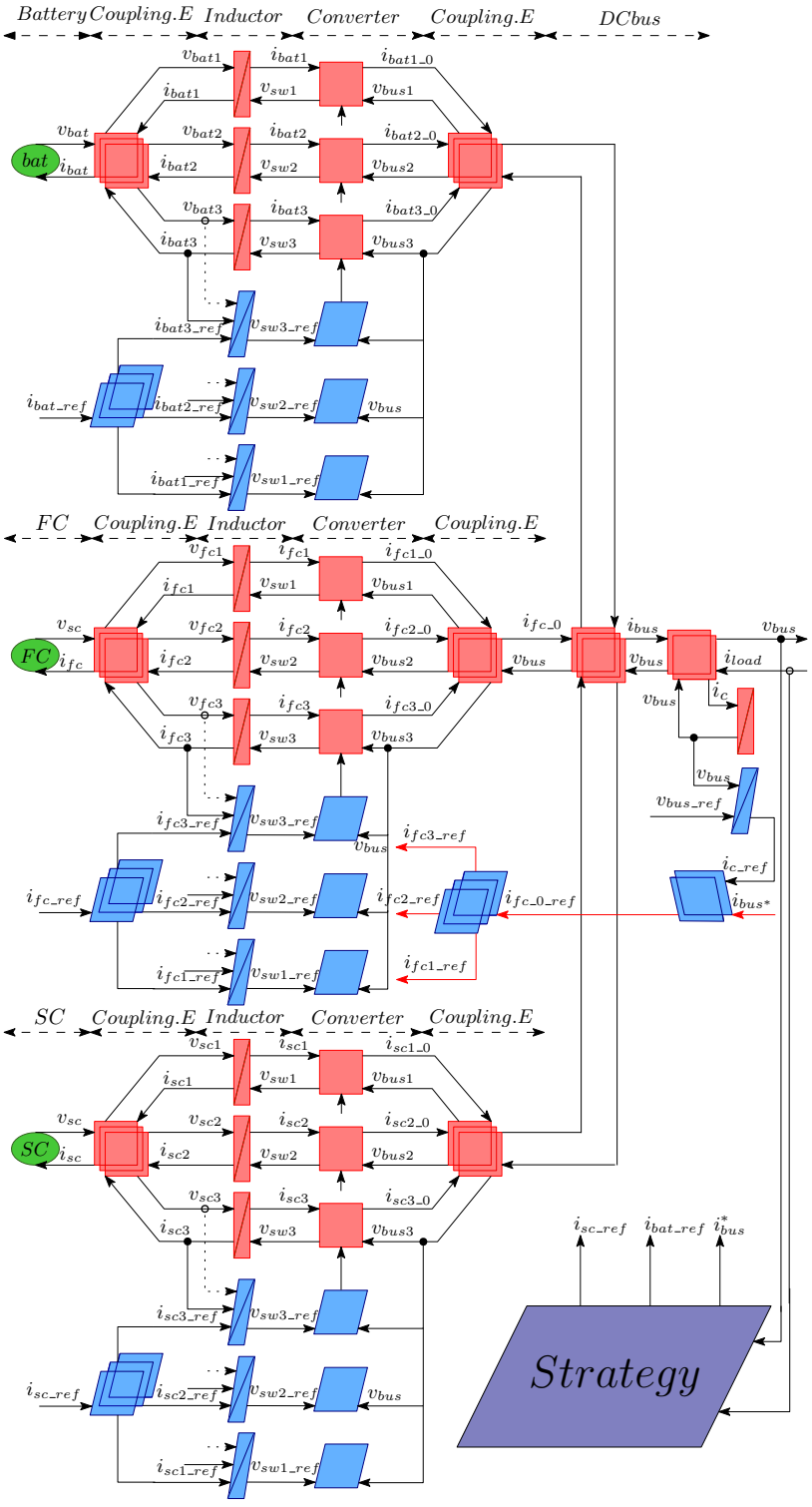

Figure 6: EMR and control structure of the electrical hybrid system

4.2. Battery and SC converters

These converters were controlled to carry out the power flow between the DC bus and the storage elements. The current of each inductor can be expressed as shown below:

$$\begin{cases} L_{bati}\dfrac{di_{bati}}{dt} = v_{bati} - v_{swi} \\ L_{sci}\dfrac{di_{sci}}{dt} = v_{sci} - v_{swi} \end{cases} \tag{6}$$

The modulation function of two IBDC converters can be expressed from the switching functions as follows:

$$\begin{cases} v_{bus} = \dfrac{1}{m_{bati}} v_{bati} \\ i_{bati} = \dfrac{1}{m_{bati}} i_{bati\_0} \end{cases} \quad \begin{cases} v_{bus} = \dfrac{1}{m_{sci}} v_{sci} \\ i_{sci} = \dfrac{1}{m_{sci}} i_{sci\_0} \end{cases} \tag{7}$$

The reference powers $P_{fc\_0\_ref}$, $P_{bat\_0\_ref}$, and $P_{sc\_0\_ref}$ can be derived from the control strategy as shown in (Figure. 5) and must be applied to the power sources when controlling the DC/DC converters. The DC bus power is defined by the following differential equation:

$$\dot{E}_{bus} = P_{fc\_0} + P_{bat\_0} + P_{sc\_0} + P_{load} \tag{8}$$

where:

$$\begin{cases} i_{fc\_ref} = \dfrac{P_{fc\_0\_ref}}{v_{fc}} \\ i_{bat\_ref} = \dfrac{P_{bat\_0\_ref}}{v_{bat}} \\ i_{sc\_ref} = \dfrac{P_{sc\_0\_ref}}{v_{sc}} \end{cases} \tag{9}$$

The control structure of the system is mainly based on reference [27, 28]. Which includes a summary for the controller design on internal model control (IMC).The latter is a method used to implement controller design, for which the resulting controller becomes directly parameterized in terms of the plant model parameters and the desired closed-loop bandwidth.

The controller transfer function is given below:

$$C(s) = \frac{\alpha^n}{(s+\alpha)^n - \alpha^n} G^{-1}(s) \tag{10}$$

With G is the plan (process), and n denotes the order of G.

4.3. DC bus voltage Controller

The DC bus voltage remains constant regardless of the required load power value. Therefore, its measurement is necessary. The voltage regulator can be designed as a PI controller

with an anti-windup block (to limit the FC current). Besides, the output signal must be limited to meet the constraints.

To define a controller, we can linearize the behavior of the system. The linearization will be carried out by an inverse model placed an opposite model of the variable i_c. It is, therefore, necessary to find an expression which allows a unit transfer between the output of the controller and the current i_c. We must set i_{fc} to the reference value that is:

$$i_{fc\_ref} = \frac{v_{bus}}{v_{fc}}(i_c + i_{bus}) \tag{11}$$

Thus, we obtain a linear relationship between $i_c(s)$ and $v_{bus}(s)$:

$$G_v(s) = \frac{v_{bus}(s)}{i_c(s)} = \frac{1}{sC} \tag{12}$$

With $G_v(s)$ is the decoupled system transfer function from i_c to v_{bus}. Based on IMC method, we can write the following relation:

$$\begin{cases} F(s) = \dfrac{\alpha_v}{s} G_v^{-1}(s) = \dfrac{\alpha_v}{s} sC \\ K_{pv} = \alpha_v C \end{cases} \tag{13}$$

For this voltage control loop, the bandwidth α_v should be smaller than the sampling frequency $F_s[Hz]$.

4.4. FC current controller

To simply define the current controller, the linearization will be made by an opposite model, we must find an expression to permit the unity transit between controller output and voltage v_{Lfci}. We must set m_{fci} to a reference value, that is:

$$m_{fci} = \frac{v_{Lfci} - v_{fc}}{v_{bus}} + 1 \tag{14}$$

Where v_{Lfci} is a new control variable representing the voltage reference across each inductor of the FC converter. We obtain a linear transfer function between $v_{Lfci}(s)$ and $i_{fci}(s)$:

$$G_{ii}(s) = \frac{i_{fci}(s)}{v_{Lfci}(s)} = \frac{1}{sL_{fci} + R_{fci}} \tag{15}$$

With $G_{ii}(s)$ is the decoupled system transfer function of each leg of the converter from v_{Lfci} to i_{fci}.

$$\begin{cases} F(s) = \dfrac{\alpha_i}{s} G_i^{-1}(s) = \dfrac{\alpha_i}{s}(sL_{fci} + R_{fci}) \\ K_{pi} = \alpha_i L_{fci} \\ K_{ii} = \alpha_i R_{fci} \end{cases} \tag{16}$$

For this inner current control loop, the bandwidth α_i should be selected smaller than a decade below the sampling frequency $F_s[Hz]$.

4.5. Battery and SC current controllers

The connection of the storage elements to the DC bus must be carried out throughout two IBDC converters, since the Battery and SC can be charged or discharged. The control of these two converters is directly linked to the EMS. These converters are controlled to supervise the power flue between the DC bus and the storage elements. For this purpose, the current references are calculated from the DC bus power and the voltage of each storage source.

The regulation carried out is a loop of current that could be able to ensure the control of the power in the converter. To be able to define a simple current regulator, we can linearize the system behavior. The linearization will be made by an opposite model, we must find an expression to permit the unity transit between controller output and voltage v_{Lbati} and v_{Lsci}. We must set m_{bati} and m_{sci} to a reference value, that is:

$$\begin{cases} m_{bati} = \dfrac{v_{Lbati} - v_{bat}}{v_{bus}} + 1 \\ m_{sci} = \dfrac{v_{Lsci} - v_{sc}}{v_{bus}} + 1 \end{cases} \tag{17}$$

We obtain a linear transfer function between $v_{Lbati}(s)$ and $i_{Lbati}(s)$ / $v_{Lsci}(s)$ and $i_{Lsci}(s)$:

$$\begin{cases} G_{bati} = \dfrac{i_{bati}(s)}{v_{Lbati}(s)} = \dfrac{1}{sL_{bati} + R_{bati}} \\ G_{sci} = \dfrac{i_{sci}(s)}{v_{Lsci}(s)} = \dfrac{1}{sL_{sci} + R_{sci}} \end{cases} \tag{18}$$

With $G_i(s)$ is the decoupled system transfer function of each leg of converters from v_{Lbati} to i_{bati} and v_{Lsci} to i_{Lsci}.

$$\begin{cases} F_{bat}(s) = \dfrac{\alpha_i}{s} G_{bati}^{-1}(s) = \dfrac{\alpha_i}{s}(sL_{bati} + R_{bati}) \\ K_{pi} = \alpha_i L_{bati} \\ K_{ii} = \alpha_i R_{bati} \end{cases} \tag{19}$$

$$\begin{cases} F_{sc}(s) = \dfrac{\alpha_i}{s} G_{sci}^{-1}(s) = \dfrac{\alpha_i}{s}(sL_{sci} + R_{sci}) \\ K_{pi} = \alpha_i L_{sci} \\ K_{ii} = \alpha_i R_{sci} \end{cases} \tag{20}$$

5. Result and discussion

First and foremost, the FC model, Battery and SC auxiliary sources, as well as the interleaved DC/DC converters with PI control of the input current and output voltage were implemented in numerical simulations. Thus, the Matlab/Simulink was adopted as the simulation tool.

The simulation was conducted to validate the proposed management strategy on a power cycle which is representative of a vehicle power demand (Figure. 1). The load requirement

consists in varying the load between two values (0 and 1700)W. We note that the rated power of the main source FC is 1500W. But, DC bus can absorb about 960W from FC power. The main idea is to activate the FC at its best efficiency when an important power is required by the vehicle. Then, the FC power will be imposed to its average value $(30-70)\%$ of its maximum power). The chosen profile of FC current is not optimal and is defined in order to highlight the current sharing between FC, battery and the SC.

(Figure. 7) shows the powers of the three sources and the load power demand. The initial state from $(t = 0to10)s$ is zero for the load, FC, Battery and SC powers, which means that the vehicle is stopped. (Figure. 9) and (Figure. 10) demonstrates that the Battery voltage v_{bat}, SC voltage v_{sc}, battery state of charge SOC_{bat} and SC state of charge SOC_{sc} are maintained around the optimal values ($v_{bat} = 26V$, $v_{sc} = 27V$, $SOC_{bat} = 75\%$, $SOC_{sc} = 85\%$), which means that the battery and SC modules are full of charge.

Beginning at $t = 7s$, the current delivered by the FC slowly increases to $18A$. The FC power will, then, be imposed to its average value (55% of its maximum power). In this case, the FC cannot satisfy the power demand of the load. Therefore, the EMS makes the Battery and SC deliver the deficit power. The auxiliary sources (Battery and SC) react immediately after each variation of the load power and behave as a high bandpass filter with a time response of a few milliseconds for SC and few seconds for Battery. When the load power is suddenly changed, the FC power slowly adjusts to the new load level as shown in (Figure. 7). During this time, it can be observed that on the Battery/SC currents shown in (Figure. 8) and powers shown in (Figure. 7), the Battery and SC react immediately to supply the transient energy demand which is not supplied by the FC.

The voltages and SOCs of the battery/SC tend to decrease, because they need to power the load when FC power is lower than the load power. However, the voltages and the SOCs of battery/SC start to increase, while the FC can provide the power and charge the Battery and SC as shown in (Figure. 9) and (Figure. 10). The battery and SC voltages varies inversely to the battery and SC currents, respectively. (Figure. 10) shows also that the variations of the Battery/SC SOCs correspond really to the battery SC voltages variations, and the variation of the SOCs is included between the min and max values imposed by the control algorithm. These values range from (60 to 75)%, for battery, and from (53 to 84)% for SC. FC voltage V_{fc} is not subject to any sudden drop related to a smooth FC current behavior i_{fc}, as shown in (Figure. 8).

Simulation results reveal the efficiency of the applied control strategy. The following key points are particularly observed.

- The Battery/SC supplies most of the transient power required by the load.
- The FC power has the slowest dynamics, while Battery/SC powers have the fastest.
- The Battery/SC SOCs are always controlled.
- The load requirements are always satisfied on the whole driving cycle.

These results demonstrate that the load demand could be met. They show, the efficiency and good performance of the control strategies. In fact, the control strategy allows achieving the main objective of energy management in the hybrid system.

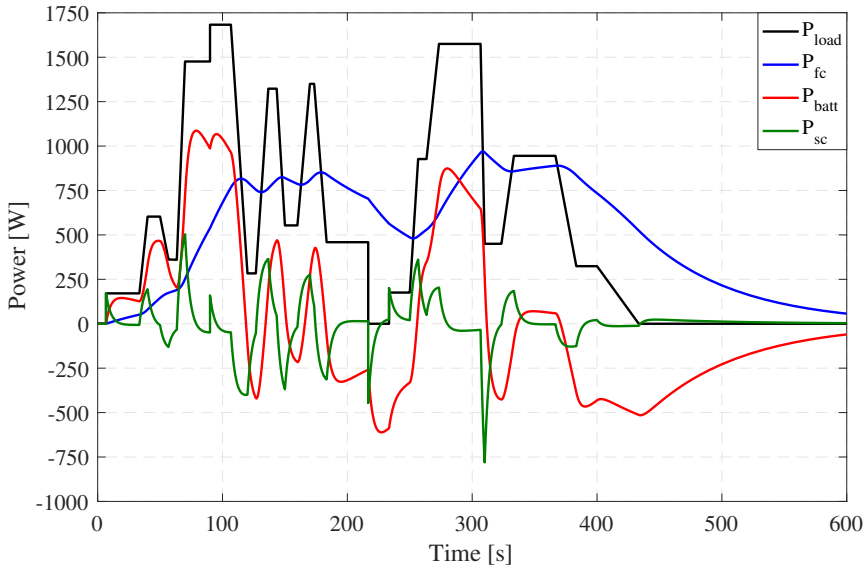

Figure 7: Load, fuel cell, Battery and SC powers.

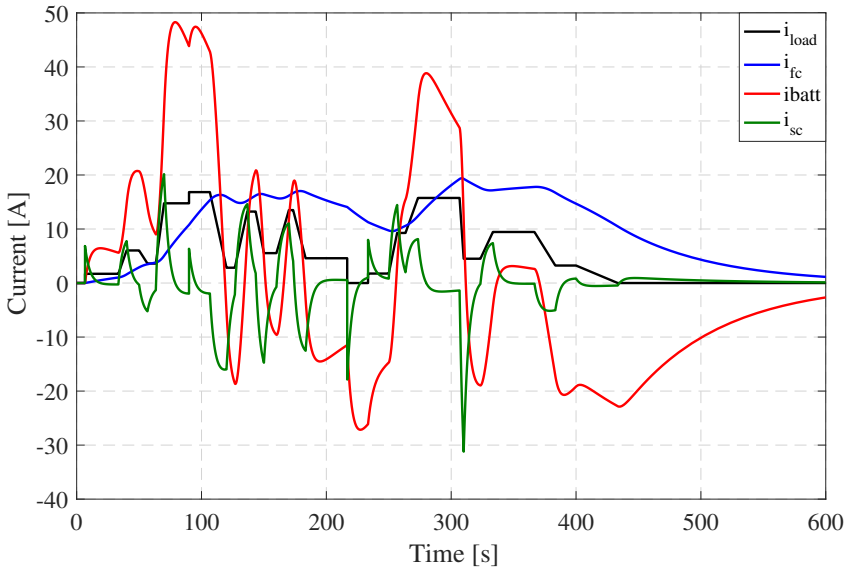

Figure 8: Load, fuel cell, Battery and SC currents

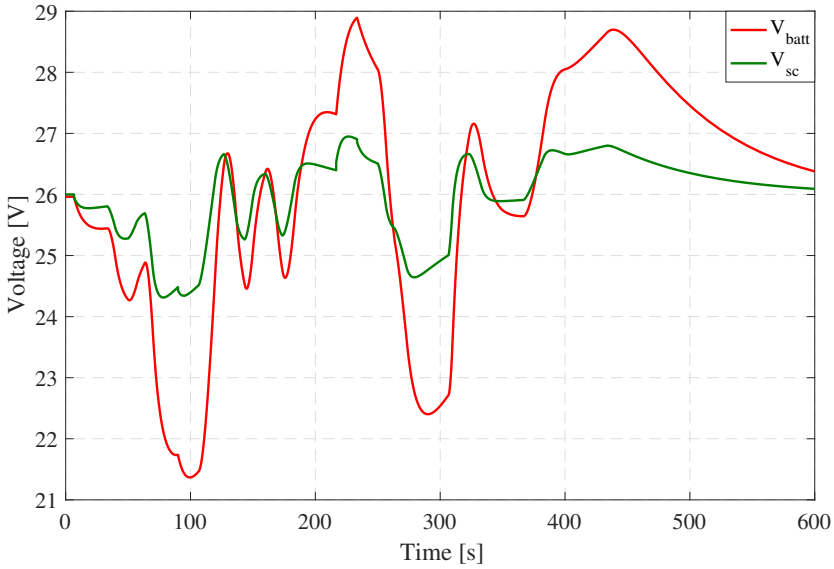

Figure 9: Battery and SC voltages

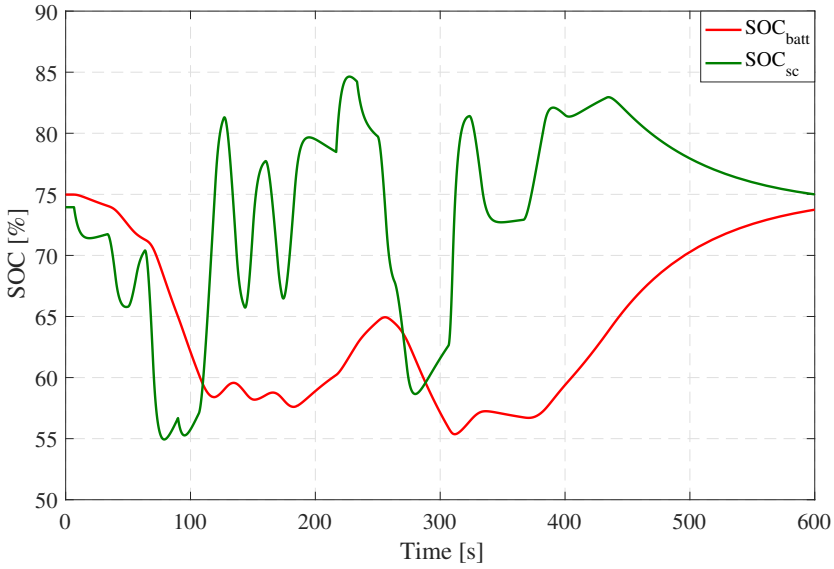

Figure 10: Battery and SC States of charge SOC

6. Conclusion

This paper dealt with the PEMFC electrical power hybridization which has already been proved to be relevant for FC lifetime enhancement. Besides, an FC/Battery/SC hybrid architecture was proposed. An EMR formulation was also used to describe the whole system (the IBC, the IBDC and the hybrid power source). In fact, our study mainly focused on the FC, Battery and SC by taking into account the intrinsic energetic characteristics of these sources (i.e. energy and power densities, typical operating dynamics) in the EMS. Simulation results showed the efficiency of the control management strategy results applied on a FC/Battery/SC system. It was also observed that the FC slow dynamic was respected using the auxiliary sources. The load requirements were always satisfied during the whole driving cycle.

References

[1] C. Wang, M. H. Nehrir, S. R. Shaw, Dynamic models and model validation for pem fuel cells using electrical circuits, IEEE Transactions on Energy Conversion 20 (2005) 442–451. doi:10.1109/TEC.2004.842357.

[2] S. Caux, J. Lachaize, M. Fadel, P. Shott, L. Nicod, Modelling and control of a fuel cell system and storage elements in transport applications, Journal of Process Control 15 (2005) 481 – 491. doi:https://doi.org/10.1016/j.jprocont.2004.08.002.

[3] H. E. Fadil, F. Giri, J. M. Guerrero, Adaptive sliding mode control of interleaved parallel boost converter for fuel cell energy generation system, Mathematics and Computers in Simulation 91 (2013) 193 – 210. doi:https://doi.org/10.1016/j.matcom.2012.07.011.

[4] B. Robyns, A. Davigny, C. Saudemont, Methodologies for supervision of hybrid energy sources based on storage systems – a survey, Mathematics and Computers in Simulation 91 (2013) 52 – 71. doi:https://doi.org/10.1016/j.matcom.2012.06.014.

[5] S. Kim, I. Hong, Effects of humidity and temperature on a proton exchange membrane fuel cell (pemfc) stack, Journal of Industrial and Engineering Chemistry 14 (2008) 357 – 364. doi:https://doi.org/10.1016/j.jiec.2008.01.007.

[6] R. Lin, F. Xiong, W. Tang, L. Técher, J. Zhang, J. Ma, Investigation of dynamic driving cycle effect on the degradation of proton exchange membrane fuel cell by segmented cell technology, Journal of Power Sources 260 (2014) 150 – 158. doi:https://doi.org/10.1016/j.jpowsour.2014.03.003.

[7] Y. Wan, J. Guan, S. Xu, Improved empirical parameters design method for centrifugal compressor in pem fuel cell vehicle application, International Journal of Hydrogen Energy 42 (2017) 5590 – 5605. doi:https://doi.org/10.1016/j.ijhydene.2016.08.162.

[8] S. B. Walker, U. Mukherjee, M. Fowler, A. Elkamel, Benchmarking and selection of power-to-gas utilizing electrolytic hydrogen as an energy storage alternative, International Journal of Hydrogen Energy 41 (2016) 7717 – 7731. doi:https://doi.org/10.1016/j.ijhydene.2015.09.008.

[9] K. Chau, 21 - pure electric vehicles (2014) 655 – 684doi:https://doi.org/10.1533/9780857097422.3.655.

[10] L. Liu, G.-Y. Kim, A. Chandra, Modeling of thermal stresses and lifetime prediction of planar solid oxide fuel cell under thermal cycling conditions, Journal of Power Sources 195 (2010) 2310 – 2318. doi:https://doi.org/10.1016/j.jpowsour.2009.10.064.

[11] H. Chen, Z. Song, X. Zhao, T. Zhang, P. Pei, C. Liang, A review of durability test protocols of the proton exchange membrane fuel cells for vehicle, Applied Energy 224 (2018) 289 – 299. doi:https://doi.org/10.1016/j.apenergy.2018.04.050.

[12] P. Piela, J. Mitzel, Polymer electrolyte membrane fuel cell efficiency at the stack level, Journal of Power Sources 292 (2015) 95 – 103. doi:https://doi.org/10.1016/j.jpowsour.2015.05.043.

[13] D. Guilbert, A. Gaillard, A. N'Diaye, A. Djerdir, Energy efficiency and fault tolerance comparison of dc/dc converters topologies for fuel cell electric vehicles (2013) 1–7doi:10.1109/ITEC.2013.6574513.

[14] A. Jaafar, C. Turpin, X. Roboam, E. Bru, O. Rallieres, Energy management of a hybrid system based on a fuel cell and a lithium ion battery: Experimental tests and integrated optimal design, Mathematics and Computers in Simulation 131 (2017) 21 – 37. doi:https://doi.org/10.1016/j.matcom.2016.01.007.

[15] N. Benyahia, H. Denoun, A. Badji, M. Zaouia, T. Rekioua, N. Benamrouche, D. Rekioua, Mppt controller for an interleaved boost dc–dc converter used in fuel cell electric vehicles, International Journal of Hydrogen Energy 39 (2014) 15196 – 15205. doi:https://doi.org/10.1016/j.ijhydene.2014.03.185.

[16] A. Payman, S. Pierfederici, F. Meibody-Tabar, B. Davat, An adapted control strategy to minimize dc-bus capacitors of a parallel fuel cell/ultracapacitor hybrid system, IEEE Transactions on Power Electronics 26 (2011) 3843–3852. doi:10.1109/TPEL.2009.2030683.

[17] J. Bauman, M. Kazerani, A comparative study of fuel-cell–battery, fuel-cell–ultracapacitor, and fuel-cell–battery–ultracapacitor vehicles, IEEE Transactions on Vehicular Technology 57 (2008) 760–769. doi:10.1109/TVT.2007.906379.

[18] C. Turpin, D. V. Laethem, B. Morin, O. Rallières, X. Roboam, O. Verdu, V. Chaudron, Modelling and analysis of an original direct hybridization of fuel cells and ultracapacitors, Mathematics and Computers in Simulation 131 (2017) 76 – 87. doi:https://doi.org/10.1016/j.matcom.2015.08.013.

[19] P. Thounthong, P. Tricoli, B. Davat, Performance investigation of linear and nonlinear controls for a fuel cell/supercapacitor hybrid power plant, International Journal of Electrical Power & Energy Systems 54 (2014) 454 – 464. doi:https://doi.org/10.1016/j.ijepes.2013.07.033.

[20] Amin, R. T. Bambang, A. S. Rohman, C. J. Dronkers, R. Ortega, A. Sasongko, Energy management of fuel cell/battery/supercapacitor hybrid power sources using model predictive control, IEEE Transactions on Industrial Informatics 10 (2014) 1992–2002. doi:10.1109/TII.2014.2333873.

[21] A. Burke, Ultracapacitors: why, how, and where is the technology, Journal of Power Sources 91 (1) (2000) 37 – 50. doi:https://doi.org/10.1016/S0378-7753(00)00485-7.

[22] W. Gao, Performance comparison of a fuel cell-battery hybrid powertrain and a fuel cell-ultracapacitor hybrid powertrain, IEEE Transactions on Vehicular Technology 54 (2005) 846–855. doi:10.1109/TVT.2005.847229.

[23] R. Dell, D. Rand, Energy storage — a key technology for global energy sustainability, Journal of Power Sources 100 (2001) 2 – 17. doi:https://doi.org/10.1016/S0378-7753(01)00894-1.

[24] C. Zheng, C. Oh, Y. Park, S. Cha, Fuel economy evaluation of fuel cell hybrid vehicles based on equivalent fuel consumption, International Journal of Hydrogen Energy 37 (2012) 1790 – 1796. doi:https://doi.org/10.1016/j.ijhydene.2011.09.147.

[25] P. Pany, R. Singh, R. Tripathi, Active load current sharing in fuel cell and battery fed dc motor drive for electric vehicle application, Energy Conversion and Management 122 (2016) 195 – 206. doi:https://doi.org/10.1016/j.enconman.2016.05.062.

[26] A. Bouscayrol, B. Davat, B. de Fornel, B. Franc cois, J. P. Hautier, F. Meibody-Tabar, M. Pietrzak-David, Multi-converter multi-machine systems:application for electromechanical drives, Eur. Phys. J. AP 10 (2000) 131–147. doi:10.1051/epjap:2000124.

[27] X. Wei, K. M. Tsang, W. L. Chan, Dc/dc buck converter using internal model control, Electric Power Components and Systems 37 (2009) 320–330. doi:10.1080/15325000802454500.

[28] K. Tarakanath, S. Patwardhan, V. Agarwal, Internal model control of dc-dc boost converter exhibiting non-minimum phase behavior (2014) 1–7doi:10.1109/PEDES.2014.7042155.